

Exotic spectroscopy at LHCb: status and prospects

Gary Robertson^{a,*} on behalf of the LHCb collaboration

^a*University of Glasgow,
Glasgow, Scotland, United Kingdom*

E-mail: gary.robertson.2@glasgow.ac.uk

The quark model predicts exotic hadrons beyond the conventional quark-antiquark mesons and three quark baryons. Exotic candidates have since been observed in the early 2000's. Since then several exotic states have been discovered. LHCb has reported on tetraquark candidates such as the $\chi_{c1}(3872)$ state, the discovery of pentaquark resonances in 2015, and the first doubly charmed tetraquark T_{cc}^+ in 2021. Many theoretical approaches, including hadronic molecules and tightly bound tetra- and penta-quarks, aim to describe the nature and properties (mass/quantum numbers) of these states, also predicting that these exotic candidates may be part of a larger multiplet of exotic states. The discovery of further exotic hadrons and measurement of their properties will help to scrutinize these theoretical models and determine the internal structure of these states. LHCb is in a unique position to study a wide range of decay modes for multiple b-hadron species. The latest results of these studies from LHCb are presented along with prospects for the Run 3 data.

*The European Physical Society Conference on High Energy Physics (EPS-HEP2023)
21-25 August 2023
Hamburg, Germany*

*Speaker

1. Introduction

Exotic hadrons - defined as hadrons with more than 3 valence quarks - were first proposed by Gell-Mann himself in his paper on the quark model [1]. Their existence was only recently confirmed in 2003 by the Belle collaboration who reported the existence of an exotic hadron named the $\chi_{c1}(3872)$ found in the $J/\psi\pi^+\pi^-$ mass spectrum [2]. Pentaquarks, which are states with 5 valence quarks, were first observed in 2015 by the LHCb collaboration in the $J/\psi p$ mass spectrum, and then most recently observed in 2019 with a larger dataset [3, 4].

These proceedings present two recent results from LHCb as well as one new result in the exotic spectroscopy field¹. These measurements benefit from the advantages of the LHCb detector, in particular the excellent particle identification (PID) capabilities.

2. Evidence of a $J/\psi K_S^0$ structure in $B^0 \rightarrow J/\psi \phi K_S^0$ decays

The $J/\psi \phi K$ mass spectrum has previously been studied by LHCb [6], where two new tetraquark states, $T_{\psi s1}^\theta(4000)^+$ and $T_{\psi s1}^\theta(4220)^+$, were observed. Another tetraquark state, the $T_{\psi s}(3985)^+$, was observed in the $D_s^+ \bar{D}^{*0}$ and $D_s^{*+} \bar{D}^0$ final states by BESIII [7]. However, the nature of these states is unknown. They could be hadronic molecules, compact tetraquarks, or some other phenomena. By searching for isospin partners to these previously established states, certain models can be favoured or disfavoured.

This work uses the full LHCb Run 1 and 2 datasets, corresponding to 9 fb^{-1} , to analyse the $B^0 \rightarrow J/\psi \phi K_S^0$ and $B^+ \rightarrow J/\psi \phi K^+$ decays. B^0 candidates are selected using a multivariate classifier. The fit to the $J/\psi \phi K_S^0$ mass spectrum is shown in Fig. 1 as well as the Dalitz plot of the final-state particles. In the $J/\psi K_S^0$ spectrum, a faint band is observed around 4 GeV. A simultaneous amplitude analysis is performed between both modes of interest in order to determine the source of the band.

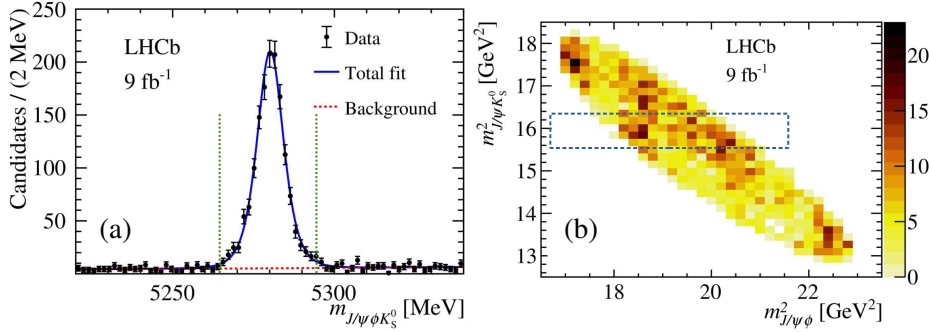


Figure 1: (a) Fit to the $J/\psi \phi K_S^0$ mass spectrum. The green dashed lines represent the mass window selected around the B^0 mass in order to produce the Dalitz plot. (b) Dalitz plot of the squared masses of $J/\psi \phi$ against $J/\psi K_S^0$ when a mass window is selected around the B^0 mass. The area of interest is highlighted with a green box.

In the amplitude fit model, components from many different sources are considered. Nine components are included in the fit for decays with an intermediate resonance from an excited kaon, $B^0 \rightarrow J/\psi(K^* \rightarrow \phi K_S^0)$. Seven components are included for decays with an intermediate unknown

¹The new LHCb naming convention is used throughout [5].

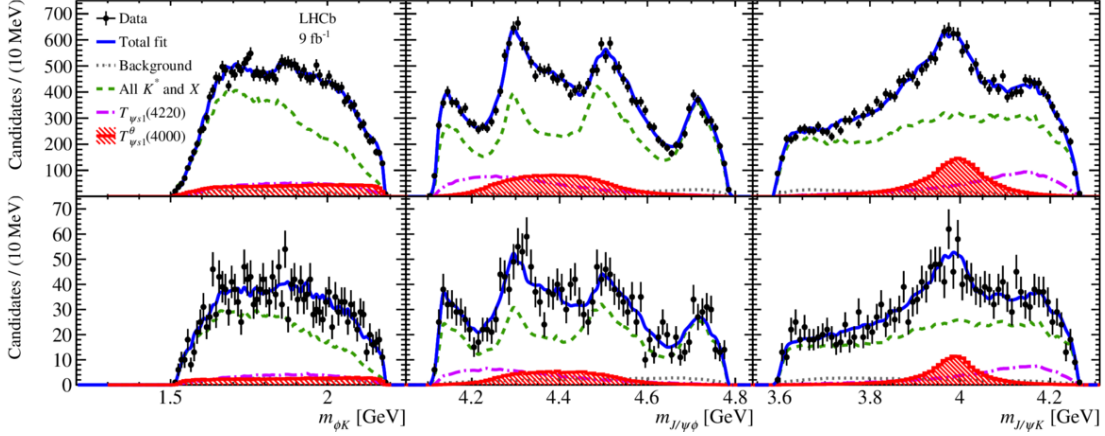


Figure 2: Distributions of (left) $m_{\phi K}$, (middle) $m_{J/\psi\phi}$, and (right) $m_{J/\psi K}$, overlaid with the corresponding projections of the default fit model. The upper and lower rows correspond to the $B^+ \rightarrow J/\psi\phi K^+$ and $B^0 \rightarrow J/\psi\phi K_S^0$ decays, respectively

Table 1: Results for the $T_{\psi_{s1}}^{\theta}(4000)^0$ state from the default model. The difference in mass between the charged and neutral states, labelled ΔM , is also given. The first uncertainty is statistical and the second systematic.

State	Mass (MeV)	Width (MeV)	ΔM (MeV)
$T_{\psi_{s1}}^{\theta}(4000)^0$	3991^{+12+9}_{-10-17}	105^{+29+17}_{-25-23}	-12^{+11+6}_{-10-4}

state, $B^0 \rightarrow (X \rightarrow J/\psi\phi)K_S^0$. Two components for the known tetraquark states $T_{\psi_{s1}}^{\theta}(4000)^+$ and $T_{\psi_{s1}}^{\theta}(4220)^+$, and a non-resonant $J/\psi\phi$ component are also included. In the default model the mass, width and helicity couplings of all fit components are identical, apart from the charged and neutral $T_{\psi_{s1}}^{\theta}(4000)$ states which are kept independent. To probe the significance of the $T_{\psi_{s1}}^{\theta}(4000)^0$ state, isospin symmetry can be assumed by fixing the couplings of these two states to the same value. For the $T_{\psi_{s1}}^{\theta}(4220)$ states the couplings are always fixed to be identical. The results of the amplitude fit are shown in Fig. 2, where sizeable components can be seen from the $T_{\psi_{s1}}^{\theta}(4000)$ and $T_{\psi_{s1}}^{\theta}(4220)$ states in both decay modes. The results from the amplitude fit for the mass, width and ΔM values for the $T_{\psi_{s1}}^{\theta}(4000)^0$ state are summarised in Table 1. ΔM represents the difference in mass of the charged and neutral $T_{\psi_{s1}}^{\theta}(4000)$ states. When including systematic uncertainties, the significance of the state is determined to be 4.0σ . In the case where the couplings are fixed between the charged and neutral $T_{\psi_{s1}}^{\theta}(4000)$ states, the significance is measured as 5.4σ . It is also seen that ΔM is consistent with zero, which also suggests the two states could be isospin partners.

3. Search for prompt production of pentaquarks in open-charm hadron final states

The pentaquark states that have been previously observed by LHCb [3, 4] have masses very close to the mass threshold of some charm baryon-meson combinations. In Fig. 3 it can be seen that, for example, the $P_c(4312)^+$ state has a mass just below the threshold of the $\Sigma_c^+ \bar{D}^0$ combination. As in the case of the previously discussed tetraquark states, the nature of these states is also not clear. They could exist as compact states, or as molecular states, or even as a charmonium-like

state. Observation of decays of these pentaquarks into charm baryon-meson final-states would help to discern which of the theories on the structure is correct, thus this work conducts a search for pentaquark decays into a range of charm baryon-meson combinations. LHCb data from 2016-2018 is used, corresponding to 5.7 fb^{-1} .

With combinations where no pentaquark signal is seen, the upper limit (UL) is set on the production ratio relative to the $\Lambda_c^+ \rightarrow pK^-\pi^+$ decay, as it is a well studied decay in LHCb. This is defined as

$$R = \frac{N_P}{N_{\Lambda_c^+}} \times \frac{\epsilon_{\Lambda_c^+}}{\epsilon_P}, \quad (1)$$

where N represents the yield of either the pentaquark signal or the Λ_c^+ , and ϵ represents the total efficiency of the selection procedure. The combinations used are shown in Fig. 3. The baryon used is either a Λ_c^+ baryon or a $\Sigma_c^{++(0)}$. The excited Σ_c states are also used in the combinations. Combinations are also selected of the decay products of the Σ_c baryons, namely the $\Lambda_c^+\pi^\pm$ decay products, allowing any potential states below threshold to be probed.

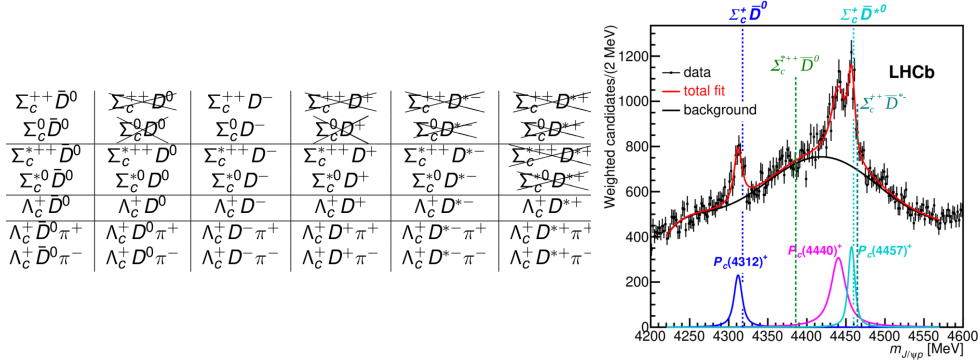


Figure 3: (left) Combinations of baryons and mesons used to search for pentaquark decays. The combinations marked with a cross are the ones which are statistically limited and have no limit set. (right) Fit to the $m_{J/\psi p}$ distribution with three Breit-Wigner amplitudes for the signal components and a sixth-order polynomial background. The mass thresholds for the for some $\Sigma_c D$ final states are superimposed.

For some combinations, there are very few events remaining in the signal region after the selections are applied. These combinations have no limit set. Each of the baryons and mesons are first optimised individually, before the optimised selections are then applied to the signal combination. A subset of the optimised baryon and meson selections are shown in Fig. 4 along with the mass windows selected around each.

The nominal signal fit is carried out simultaneously to the signal and sideband regions, where the sideband is defined as a high mass and low mass window around either the Λ_c^+ or Σ_c baryon, where no signal is expected. No significant signal is seen in any combinations. The highest global significances found are 2.56σ and 2.35σ in the $\Lambda_c^+\pi^-\bar{D}^0$ and $\Lambda_c^+\pi^-D^-$ combinations respectively, and the result of the fit for each is shown in Fig. 5. The variation of the p -value found when scanning the mass spectrum for the $\Lambda_c^+\pi^-\bar{D}^0$ combination is also shown in Fig. 6. The previously observed pentaquark states are also investigated, namely the $P_c(4312)^+$, $P_c(4440)^+$ and $P_c(4457)^+$

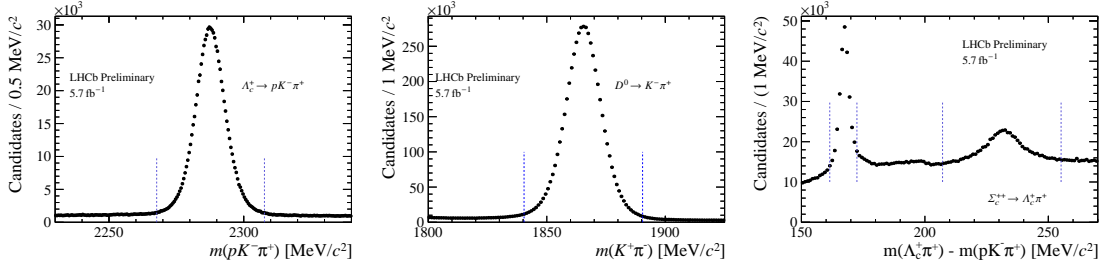


Figure 4: Invariant mass distributions are shown for the (left) $\Lambda_c^+ \rightarrow p K^- \pi^+$, (middle) $D^0 \rightarrow K^- \pi^+$, (right) $\Sigma_c^{(*)++} \rightarrow \Lambda_c^+ \pi^+$ decays. Note that in the right plot the mass of the resonant final-state particle is subtracted from the mass distribution to minimise detector resolution effects. The blue dashed lines show the chosen signal windows around the peaks.

states. This is only carried out for states with the same total charge and hidden charm quark content. By setting the mass and width of the signal model to the known values of these states [4] and carrying out the same fitting procedure previously described, the significance of the states is found. The significance in these spectra is found to be zero in all cases, thus limits are set using the same procedure. Since the mass of the pentaquarks in the spectrum of the combinations is not certain,

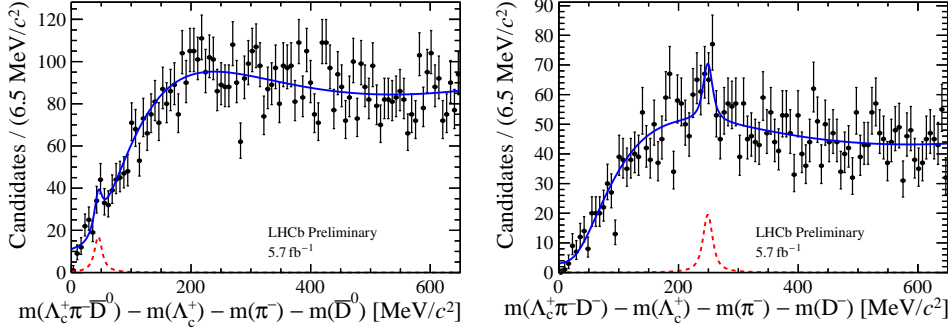


Figure 5: Fit result for the most significant signal seen in the (left) $\Lambda_c^+ \pi^- \bar{D}^0$, and (right) $\Lambda_c^+ \pi^- D^-$ modes, where the data are represented by black dots, the total fit by the solid blue line and the signal fit by the dashed red line.

the UL is found in steps of $4 \text{ MeV}/c^2$ from the kinematic mass threshold to $600 \text{ MeV}/c^2$ above. The UL is then smeared by a Gaussian function, where the width of the Gaussian is fixed to the total systematic uncertainty. An example of the UL found when scanning across the mass spectrum is shown in Fig. 6. The combinations with the highest global significances give hints that more states could be discovered in these spectra when a larger LHCb dataset is available.

4. Observation of the $B_s^0 \rightarrow \chi_{c1}(3872) \pi^+ \pi^-$ decay

Although the $\chi_{c1}(3872)$ state was the first exotic hadron state to be discovered its nature is still unclear, namely whether it is a true charmonium state or a bound $D^{*0} \bar{D}^0$ state. Additional measurements of $\chi_{c1}(3872)$ production in B decays will help to discern the nature of the state. For example, the observed difference in $\mathcal{B}(B^+ \rightarrow \chi_{c1}(3872) K^+)$ and $\mathcal{B}(B^0 \rightarrow \chi_{c1}(3872) K^0)$ [8]

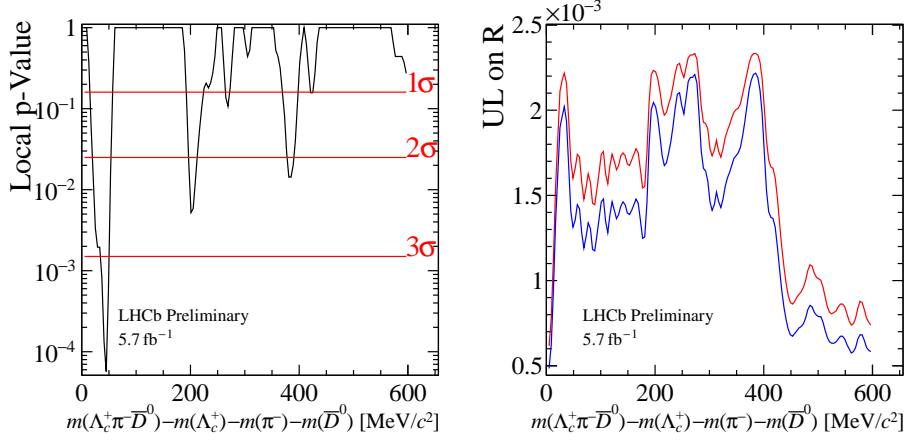


Figure 6: (left) Local p -value distributions for the $\Lambda_c^+\pi^-\bar{D}^0$ combination, (right) Upper limit on the R distribution, with the 90% CL in blue and the 95% CL in red, for the $\Lambda_c^+\pi^-\bar{D}^0$ combination.

could be explained by the $\chi_{c1}(3872)$ state being a compact tetraquark. In this work the branching fraction of the $B_s^0 \rightarrow \chi_{c1}(3872)\pi^+\pi^-$ decay relative to the $B_s^0 \rightarrow \psi(2S)\pi^+\pi^-$ decay, where both the $\chi_{c1}(3872)$ and $\psi(2S)$ states decay to a dipion final state, is measured using the full Run 1 and 2 dataset, corresponding to 9 fb^{-1} . The ratio between the two is found in the same method as defined by Eq. 1. Since the final state of both decays is four charged pions, the systematic uncertainties are greatly simplified since many will cancel in the ratio.

For the fit to the signal region, a simultaneous fit is carried out to both the $J/\psi\pi^+\pi^+\pi^-\pi^-$ and $J/\psi\pi^+\pi^-\pi^-\pi^-$ spectra, in both the $\chi_{c1}(3872)$ and $\psi(2S)$ mass regions. For the $\chi_{c1}(3872)$ state, there are four components in the fit; one for the $B_s^0 \rightarrow \chi_{c1}(3872)\pi^+\pi^-$ decay which is the signal component, one for the $B_s^0 \rightarrow J/\psi\pi^+\pi^+\pi^-\pi^-$ decay where the $J/\psi\pi^+\pi^-$ combination does not originate from a $\chi_{c1}(3872)$ decay, one for random combinations of the $\chi_{c1}(3872)$ with two pions representing the combinatorial background from the dipion pair, and one for fully random combinations of $J/\psi\pi^+\pi^+\pi^-\pi^-$ representing the fully combinatorial background. The same components are also defined for the $\psi(2S)$ state. The results of the fit for both mass regions are shown in Fig. 7. The

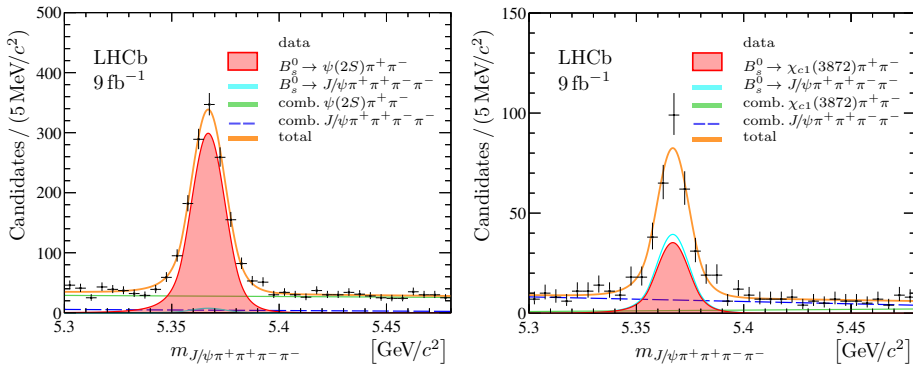


Figure 7: Distributions of the $J/\psi\pi^+\pi^+\pi^-\pi^-$ mass of (left) $B_s^0 \rightarrow \psi(2S)\pi^+\pi^-$ (right) $B_s^0 \rightarrow \chi_{c1}(3872)\pi^+\pi^-$ candidates with the fit results overlaid.

yields are found to be $N_{\psi(2S)} = 1301 \pm 47$ and $N_{\chi_{c1}(3872)} = 155 \pm 23$ and the significance of the

$B_s^0 \rightarrow \chi_{c1}(3872)\pi^+\pi^-$ decay when including systematic uncertainties is measured as 7.3σ . The branching fraction relative to the $\psi(2S)$ channel is thus measured as $R = (6.8 \pm 1.1 \pm 0.2) \times 10^{-2}$ where the first error is statistical and the second is systematic. A large contribution in the dipion system is also seen from the $f_0(980)$ state, but further study is needed to fully understand this.

5. Conclusion

Many new exotic hadrons have been discovered recently, many of which have been reported by LHCb. In these proceedings the evidence of a new tetraquark state which is an isospin partner of the existing $T_{\psi s 1}^\theta(4000)^+$ state has been summarised, as well as the search for a range of pentaquark states decaying into charm baryon-meson combinations. A new observation of a B decay involving the $\chi_{c1}(3872)$ state has also been discussed. All of these works will be important to their respective areas of research, and the results will be used to guide future studies. There are still many results to come from the current LHCb dataset in the next few years, as well as many more results to come from upcoming runs (for example Run 3 and Run 4 will collect 50 fb^{-1} in total). Current and future upgrades will also improve the detector such that analysts are able to fully exploit its capabilities, *e.g.* an improved trigger will lead to cleaner hadronic events and higher sensitivity.

References

- [1] M. Gell-Mann, *A schematic model of baryons and mesons*, Phys. Lett. **8**, 214 (1964), doi:[10.1016/S0031-9163\(64\)92001-3](https://doi.org/10.1016/S0031-9163(64)92001-3).
- [2] Belle Collaboration, S.-K. Choi *et al.*, *Observation of a Narrow Charmonium-like State in Exclusive $B^\pm \rightarrow K^\pm\pi^+\pi^-J/\psi$ Decays*, PRL **91**, 262001 (2003), doi:<https://doi.org/10.1103/PhysRevLett.91.262001>.
- [3] LHCb Collaboration, R. Aaij *et al.*, *Observation of $J/\psi p$ Resonances Consistent with Pentaquark States in $\Lambda_b^0 \rightarrow J/\psi K^- p$ Decays*, PRL **115**, 072001 (2015), doi:<https://doi.org/10.1103/PhysRevLett.115.072001>.
- [4] LHCb Collaboration, R. Aaij *et al.*, *Observation of a Narrow Pentaquark State, $P_c(4312)^+$, and of the Two-Peak Structure of the $P_c(4450)^+$* , PRL **122**, 222001 (2019), doi:<https://doi.org/10.1103/PhysRevLett.122.222001>.
- [5] LHCb Collaboration, R. Aaij *et al.*, *Exotic hadron naming convention*, arXiv:2206.15233 [hep-ex], doi:<https://doi.org/10.48550/arXiv.2206.15233>.
- [6] LHCb Collaboration, R. Aaij *et al.*, *Observation of New Resonances Decaying to $J/\psi K^+$ and $J/\psi \phi$* , PRL **127**, 082001 (2021), doi:<https://doi.org/10.1103/PhysRevLett.127.082001>.
- [7] BESIII Collaboration, M. Ablikim *et al.*, *Observation of a Near-Threshold Structure in the K^+ Recoil-Mass Spectra in $e^+e^- \rightarrow K^+(D_s^+D^{*0} + D_s^{*+}D^0)$* , PRL **126**, 102001 (2021), doi:<https://doi.org/10.1103/PhysRevLett.126.102001>.
- [8] Belle Collaboration, H. Hirata *et al.*, *Study of the lineshape of $\chi_{c1}(3872)$ using B decays to $D^0\bar{D}^{*0}K$* , PRD **107**, 112011 (2023), doi:<https://doi.org/10.1103/PhysRevD.107.112011>.